Title
Bortezomib Improves Adoptive T-cell Therapy by Sensitizing Cancer Cells to FasL Cytotoxicity

Journal
Cancer Research, 75(24)

ISSN
0008-5472

Authors
Shanker, Anil
Pellom, Samuel T
Dudimah, Duafalia F
et al.

Publication Date
2015-12-15

DOI
10.1158/0008-5472.can-15-0794

Peer reviewed

HHS Public Access
Author manuscript
Cancer Res. Author manuscript; available in PMC 2016 December 15.

Published in final edited form as:
Cancer Res. 2015 December 15; 75(24): 5260–5272. doi:10.1158/0008-5472.CAN-15-0794.

Bortezomib improves adoptive T cell therapy by sensitizing cancer cells to FasL cytotoxicity

Anil Shanker[1,2,3], **Samuel T Pellom Jr**[1,3,4], **Duafalia F Dudimah**[1], **Menaka C Thounaojam**[1], **Rachel L de Kluyver**[5], **Alan D Brooks**[5,6], **Hideo Yagita**[7], **Daniel W McVicar**[5], **William J Murphy**[8], **Dan L Longo**[9], and **Thomas J Sayers**[5,6]

[1]Department of Biochemistry and Cancer Biology, School of Medicine, Meharry Medical College, Nashville, TN

[2]Host-Tumor Interactions Research Program, Vanderbilt-Ingram Cancer Center, Vanderbilt University, Nashville, TN

[3]School of Graduate Studies and Research, Meharry Medical College, Nashville, TN

[4]Department of Microbiology and Immunology, School of Medicine, Meharry Medical College, Nashville, TN

[5]Cancer and Inflammation Program, National Cancer Institute, Frederick, MD

[6]Basic Sciences Program, Leidos Biomedical Research, Inc., Frederick, MD

[7]Department of Immunology, Juntendo University School of Medicine, Tokyo, Japan

[8]Division of Hematology/Oncology, Departments of Dermatology and Internal Medicine, University of California School of Medicine, Davis, CA

[9]Laboratory of Genetics and Genomics, National Institute on Aging, National Institutes of Health, Baltimore, MD

Abstract

Cancer immunotherapy shows great promise but many patients fail to show objective responses, including in cancers that can respond well such as melanoma and renal adenocarcinoma. The proteasome inhibitor bortezomib sensitizes solid tumors to apoptosis in response to TNF-family death ligands. Since T cells provide multiple death ligands at the tumor site, we investigated the

Correspondence to: Anil Shanker, PhD, Laboratory of Lymphocyte Function, Department of Biochemistry and Cancer Biology, Meharry Medical College School of Medicine, 2005 Harold D. West Basic Sciences Building, 1005 Dr DB Todd Jr Boulevard, Nashville, TN 37208 USA. Tel. 615-327-6460, Fax 615-327-6442, ashanker@mmc.edu; and Thomas J Sayers, PhD, P.O. Box B, Frederick, MD 21702 USA. Tel 301-846-5729, Fax 301-846-1673; sayerst@mail.nih.gov.

Disclosure of Potential Conflicts of Interest
No potential conflicts of interest.

Authors' Contributions
Conception and design: A.S., T.J.S.
Development of methodology: A.S., A.D.B.
Acquisition of data: A.S., S.T.P., D.F.D., M.C.T., R.L. de K.
Analysis and interpretation of data (e.g., statistical analysis, biostatistics, computational analysis): A.S., TJS
Writing, review, and/or revision of the manuscript: A.S., S.T.P., M.C.T., R.L. de K., H.Y., D.W.McV., W.J.M., D.L.L., T.J.S.
Administrative, technical, or material support (i.e., reporting or organizing data, constructing databases): A.S., T.J.S.
Study supervision: A.S., T.J.S.

effects of bortezomib on T cell responses in immunotherapy models involving low-avidity antigens. Bortezomib did not affect lymphocyte or tissue-resident $CD11c^+CD8^+$ dendritic cell counts in tumor-bearing mice, did not inhibit dendritic cell expression of co-stimulatory molecules and did not decrease MHC class I/II-associated antigen presentation to cognate T cells. Rather, bortezomib activated NF-κB p65 in $CD8^+$ T cells, stabilizing expression of T cell receptor CD3ζ and IL-2 receptor-α, while maintaining IFN-γ secretion to improve FasL-mediated tumor lysis. Notably, bortezomib increased tumor cell surface expression of Fas in mice as well as human melanoma tissue from a responsive patient. In renal tumor-bearing immunodeficient $Rag2^{-/-}$ mice, bortezomib treatment after adoptive T cell immunotherapy reduced lung metastases and enhanced host survival. Our findings highlight the potential of proteasome inhibitors to enhance antitumor T cell function in the context of cancer immunotherapy.

Introduction

The proteasome is an essential component of the cellular protein degradation machinery. The greater dependence of cancer cells on the proteasome to remove aberrant proteins compared with nonmalignant cells, as well as the reliance of various tumors on the proteasome-dependent NF-κB activation pathway to maintain resistance to apoptosis, makes cancer cells selectively more susceptible to proteasome inhibitors (1). Bortezomib (Velcade/PS-341) is a dipeptidyl boronate proteasome inhibitor that has been approved by the US Food and Drug Administration for the treatment of multiple myeloma (2) and mantle cell lymphoma (3) and its use has been extended to advanced stage non-small cell lung cancer (4). As shown by us and others, Bortezomib sensitizes solid tumor cells to TRAIL or its receptor agonist mAb by amplifying tumor cell caspase-8 activation in the death-inducing signaling complex following death receptor ligation (5-8). However, as a single agent bortezomib is ineffective in most solid cancers, and there are concerns in combining bortezomib with adoptive T-cell therapy because of reports purporting immunosuppressive actions of bortezomib (9,10). Indeed, concerns over the possible side effects of bortezomib on immune effector functions have been raised recently (11-15). On the other hand, there are a number of reports indicating that bortezomib either directly or indirectly can play a positive therapeutic role in amplifying immune antitumor effector functions (16-22). Nonetheless, to date there has been no systematic study of the effects of bortezomib on adoptive cellular immunotherapy (ACT) in mouse preclinical cancer models *in vivo*.

Studies using the influenza viral hemagglutinin (HA) expressed as a model tumor antigen (Ag) in a renal cell carcinoma (RencaHA), as well as a self-Ag in pancreatic islet β-cells in insulin-HA transgenic mice, showed that host T-cells could react to a self low-avidity epitope of HA and reject HA-expressing tumor cells without inducing autoimmune diabetes (23). Taking advantage of this low-avidity model antigen and the availability of MHC class I and II–restricted HA-specific T-cell receptor (TCR)–transgenic Cln4 and $6.5^{+/+}$ mice, respectively (23,24), we investigated the effects of bortezomib administration on T-cell responses in an adoptive T-cell transfer setting in mice with established renal RencaHA or mammary 4T1.2HA adenocarcinoma tumors. We compared the effects in two distinct *in vivo* protocols, one tumor therapeutic regimen of bortezomib (Bzb-T) standardized by us earlier(7) with another known suppressive regimen of bortezomib (Bzb-S) close to the maximal tolerated levels for this drug. The suppressive Bzb-S regimen was adapted from Sun *et al*'s study, where bortezomib suppressed acute lethal graft-versus-host (GVHD) response in myeloablated mice following allogenic bone marrow transfer (10).

Surprisingly, adoptive T-cell transfer followed by bortezomib administration resulted in reduced numbers of lung metastatic tumor nodules and enhanced survival of tumor-bearing mice when compared with either treatment alone. The therapeutic regimen of bortezomib we used in this study had no major effect on the number of $CD4^+$ or $CD8^+$T lymphocytes, or tissue-resident $CD11c^+CD8^+$ dendritic cells (DC) in tumor-bearing mice, nor did it affect the expression of costimulatory molecules, or decrease the MHC class I or II–associated antigen presentation to HA-specific T-cells. Rather, sustained T-cell function *in vivo*, evident by various functional readouts, following adoptive T-cell transfer combined with the therapeutic regimen of bortezomib efficiently cleared tumors predominantly by the FasL pathway. Moreover, a high surface expression of Fas was observed on tumor cells in bortezomib-administered mice, and on human melanoma tissue from a responsive patient following a combination therapy that included bortezomib. Taken together, these findings illustrate the clinical potential of using appropriate timing and dosing of bortezomib administration for sensitizing cancer cells to T-cell-mediated killing, stabilizing T-cell activation, and thereby improving the outcome of adoptive T-cell therapy of cancer.

Methods

Mice—BALB/c and recombination-activating-gene-$2^{-/-}$ ($RAG2^{-/-}$) mice (7–12-week) were bred at the National Cancer Institute (NCI)-Frederick, or at Meharry Medical College. TCR transgenic Cln4 mice were provided by Linda A. Sherman, The Scripps Research Institute, La Jolla, CA. Cln4 mice were established on $RAG2^{-/-}$, $Pfp^{-/-}$ and gld.gld backgrounds. TCR transgenic $6.5^{+/+}$ mice were provided by Hyam I. Levitsky, John Hopkins University, Baltimore, MD. TCR transgenic mice were genotyped according to the methods described earlier (23,25). Mice were cared for in accordance with the procedures outlined in the National Institutes of Health *Guide for the Care and Use of Laboratory Animals.* NCI-Frederick and Meharry Medical College are accredited by the Association for Assessment and Accreditation of Laboratory Animal Care International and follow the Public Health Service Policy for the care and use of laboratory animals under pathogen-free conditions.

Cell lines—The RencaHA line (courtesy Hyam I. Levitsky), 4T1.2 (courtesy Suzanne Ostrand-Rosenberg, University of Maryland, Baltimore, MD), and C26 and A20 (ATCC, Manassas, VA) were maintained in FCS-supplemented standard RPMI-1640 culture medium. We regularly go back to reference stocks to ensure fidelity; routine sterility and mycoplasma testing are performed regularly. Low-passage (< 5) tumor cell cultures were used for the experiments.

Human melanoma tissues—Paraffin-embedded melanoma tissue sections were provided by Ann Richmond and Jeffrey A Sosman, Vanderbilt University Medical Center, Nashville, TN. They were collected in a phase I clinical trial (26) that included nineteen histologically proven, advanced-stage (III or IV) metastatic melanoma patients (17 M1c, 10 elevated lactate dehydrogenase, 12 ECOG performance status 1-2) enrolled onto escalating dose levels of temozolomide (50-75 mg/m^2) daily, orally, for 6 of 9 weeks and bortezomib (0.75-1.5 mg/m^2) by i.v. push on days 1, 4, 8, and 11 of every 21-d cycle. Twelve paired melanoma tissue samples collected on day 0 before treatment and on days 8-45 after treatment were analyzed for Fas immunostaining.

Tumor monitoring—Mice injected with tumor cells were monitored weekly for the relevant outcome (i.e., tumor metastasis or survival). Tumor metastatic nodules in mice intravenously injected with RencaHA cells were counted under a dissection microscope on the surgically-removed lungs, fixed in Bouin's fluid.

T-cell adoptive transfer—The naive HA-specific monoclonal CD8 T-cells were obtained from the lymph node (LN) cells or red blood cell (RBC)-depleted splenocytes of Cln4 RAG2$^{-/-}$ mice. They were washed and injected intravenously in tumor-bearing RAG2$^{-/-}$ mice. In some experiments, a hamster neutralizing antibody to FasL (MFL4) or a control isotype antibody (UC8-1B9) (generated at Juntendo University, Japan) was injected i.v. at 0.5 mg/mouse on days 7 and 10 following injection of RencaHA cells.

Immunoblotting

CD8$^+$ T cells were purified from splenocytes by incubating cells with rat anti-mouse CD8 mAb, followed by positive selection of CD8$^+$ cells with anti-rat IgG Microbeads (Miltenyi Biotec) and cell pellets were lysed in complete lysis buffer including protease and phosphatase inhibitors. Nuclear and cytoplasmic extracts were prepared using Ne-per nuclear and cytoplasmic extraction reagent (Life Technologies). Fifty micrograms of each protein sample was electrophoresed on NuPage 4-12% Bis-Tris gel (Novex Life Technologies) and transferred to polyvinylidenedifluoride membranes using an iBlot® Dry Blotting system (Life Technologies). The membrane was then blocked in 5% skimmed milk in 1X PBS-Tween-20 (1X PBST) for 2 h at room temperature with gentle agitation. After blocking, the blots were incubated with rabbit anti-mouse antibodies against total and phosphorylated protein of p65 (Total D14E12; Phospho S468; Cell Signaling) in 1% BSA (in 1X PBST) overnight at 4°C with gentle agitation. After five washes of 5 minutes each in 1X PBST, blots were incubated with goat anti-rabbit horseradish peroxidase (Santa Cruz Biotechnology, CA) at a dilution of 1:4000 in 1X PBST for 1.5 h, with agitation. The blots were rinsed again in 1X PBST, and developed by using chemiluminescence reagent (Millipore, MA) and a Kodak Image Station (Kodak, Rochester, NY). The blots were then stripped and probed with HRP conjugated anti-GAPDH antibody (Cell Signaling Technologies, MA) to determine equivalent loading.

Immunohistochemistry—The immunohistochemical analyses of murine RencaHA solid tumors, thymus, or lungs were performed according to standard methods (27). Digital images of the specimens were captured using Spectrum image software (Aperio Technologies, Inc., Vista, CA). For human melanoma tissues embedded in paraffin, 6-μm-thick sections were cut, deparaffinized and hydrated before treating for antigen retrieval with sodium citrate buffer for 20 min. Lab Vision Autostainer360 was used for staining using Ultravision Quanto Detection System HRP DAB kit (#TL-060-QHD). In brief, tissues were treated with peroxidase followed by UV block before treating with primary anti-human/

mouse CD95/FAS (LS-B6851/33954) at 1:200 for 45 min. Tissues were then treated with labeled horse radish peroxidase and stained with 3,3'-diaminobenzidine for 5 min. Counter staining was done with Hematoxylin, dehydrated and mounted in cytoseal. For negative control, tissues were stained with isotype IgG.

Proteasome inhibition assay—Red blood cell-depleted splenocytes, LN, lung or excised tumor mass cells were prepared from mice at different time points after last bortezomib administration. Cells were plated in white 96-well plates at 1×10^4 cells per well and assayed using the Proteasome-Glo Chymotrypsin-Like Cell-Based Assay (Promega) according to the manufacturer's protocol.

Flow cytometry—Cells were stained for surface immunofluorescence staining with various antibodies or control isotypes (BD Biosciences, San Jose, or eBioscience Inc., San Diego, CA) following FcγR-blocking. Anti-hemagglutinin clone H28-E23 was obtained from Jonathan W Yewdell (NIAID, Bethesda, MD) and was used with secondary sheep anti-mouse IgG biotin and straptavidin-APC. IFN-γ or CD3ζ intracellular staining was measured in T-cells isolated from the tumor and the draining lymph nodes following *ex vivo* re-stimulation for 5 h with 200 ng/ml ionomycin plus 10 ng/ml phorbol 12-myristate 13-acetate (Sigma, St. Louis, MO) in the presence of GolgiStop™ protein transport inhibitor (BD Biosciences) as per manufacturer's protocol. Data were acquired on leukocyte gates as per forward and side scatters using a FACS Calibur or LSR-I flow cytometer (BD Biosciences) or Guava EasyCyte HT system (EMD Millipore) and analyzed using CellQuest (BD Biosciences) or FlowJo (Treestar Inc., CA) softwares.

T-cell proliferation—T-cell divisions were measured by flow cytometry using the intracytoplasmic stable carboxyfluorescein succinimidyl ester (CFSE) dye that exhibits sequential halving of intracellular fluorescence intensity at each division step. TCRHA $CD8^+$ T-cells were incubated for 10 min at 37°C with 5 μM CFSE (Molecular Probes) and injected i.v. (2 to 5×10^6 per mouse) in $RAG2^{-/-}$ recipients at the indicated times after RencaHA injection. CFSE-labeled TCRHA $CD8^+$ T-cells were analyzed *ex vivo* from tumor-draining LNs, contralateral LNs or spleens on indicated days after transfer. In an *in vitro* set up, CD11c-labelled magnetic bead-purified cells from various groups of mice were irradiated, and pulsed for 2 h with HA peptide or with HA protein along with a cationic Pro-Ject delivery reagent (Pierce), and washed. Equal numbers of these HA-pulsed $CD11c^+$ cells were co-cultured with CFSE-labeled $RAG2^{-/-}$Cln4 TCRHA $CD8^+$ T-cells for 3 days before analysis of CFSE division profiles or intracellular IFN-γ secretion.

CTL generation—CTL were generated from the LN cells of Cln4 $RAG2^{-/-}$ mice, stimulated *in vitro* for 3 d with lipopolysaccharide-treated (15 μg/mL) irradiated syngeneic wild-type RBC-depleted splenocytes loaded with 10^{-6} M $HA_{518\text{-}526}$ (IYSTVASSL) or an irrelevant nucleoprotein (TYQRTRALV) peptide. On day 3, cells were washed and used for cytolytic assay. To determine the necessary effector mechanism of activated T-cells, CTL were generated *in vitro* from Cln4 $RAG2^{-/-}$, Cln4 $Pfp^{-/-}$ and Cln4 gld.gld mice and 5×10^6 CTLs/mouse were injected i.v. on day 10 after the injection of RencaHA cells (2×10^6/mouse , i.v.) in $RAG2^{-/-}$ mice.

Cytolytic assay *in vivo*—Syngeneic splenocytes were labeled *in vitro* with 10^{-6}M $HA_{518-526}$ or an irrelevant nucleoprotein (TYQRTRALV) peptide. The splenic targets were labeled with high concentration of CFSE (0.5 μM) or low concentration of CFSE (0.1μM), respectively, and were mixed in 1:1 ratio. Labeled target cells were injected intravenously in experimental WT mice (5×10^6 per mouse) following bortezomib (1mg/kg body weight) and TCRHA Cln4 CD8 T CTL (1×10^7 per mouse) intravenous administration and harvested 16 h later from the spleen or tumor-draining lymph nodes for analysis by flow cytometry. The ratio of HA-expressing to irrelevant target cells was calculated to quantify specific target clearance.

Specific lysis—Target tumor cells, pulsed with HA peptide (10^{-6}M) for 90 min at 37 °C, radio-labelled with ^{111}In-labeled oxyquinoline (Amersham Health, Medi-Physics Inc., Arlington Heights, IL), and washed, were incubated for 18 h with CTL effectors. After overnight incubation, supernatants were harvested and counted on a 1480 Wizard 3 automatic γ-counter (Perkin Elmer Life and Analytical Sciences, Shelton, CT). Percent cytotoxicity was calculated as described previously (28).

Cell counts and viability—Cell preparations from the LN, spleen and blood were subjected to automated hematology analysis (KX-21, Sysmex Corporation, Kobe, Japan), and total numbers of white blood cells, and lymphocytes were enumerated. In some experiments, viable cells were quantified by measuring absorbance at 490 nm following 3-[4,5-dimethyiazol-2-yl-5]-[3-carboxymethyloxyphenyl]-2-[4-sulfophenyl]-2H tetrazolium (MTS) (Promega, Madison, WI) assay described previously (20). The percentage decrease in cell number is calculated as 1 − [absorbance of treated cells − absorbance of media] / [absorbance of untreated cells − absorbance of media] × 100%.

Statistics—Comparisons of mean values between the groups were analyzed using GraphPad Instat software (GraphPad Prism). Statistical significance of the differences was analyzed by using unpaired Student *t* test or by analysis of variance (ANOVA). Comparisons of survival curves estimated by Kaplan-Meïer plots using GraphPad Prism were performed by the log-rank (Mantel-Cox) test. All statistical tests were two-sided, with p-values < 0.05 considered statistically significant.

Results

Effects of therapeutic and suppressive regimens of bortezomib on endogenous leukocyte numbers

We have previously reported that the proteasome inhibitor bortezomib (Velcade/PS-341) sensitizes solid tumors, such as renal or mammary adenocarcinoma cells to apoptosis in response to TNF-family death ligands or TRAIL receptor agonist mAb by amplifying caspase 8 activation in the death-inducing signaling complex, which translates into a survival benefit in tumor-bearing mice (7,8). To address concerns over the possible side effects of bortezomib on immune functions, we tested two *in vivo* protocols with opposite effects on tumor burden and survival. The low intensity tumor therapeutic regimen of bortezomib, Bzb-T, given twice a week (7) was compared with a previously described suppressive regimen of bortezomib, Bzb-S, given four times a week close to the maximal tolerated levels that suppressed acute lethal GVHD response in myeloablated mice following allogenic bone marrow transfer (10). Proteasome activity was determined following bortezomib administration as per the two regimens (**Fig 1A)** in WT mice injected with RencaHA tumor cells subcutaneously. At 4 h after last bortezomib administration, the cellular proteasome activity in spleen, tumor-draining LN and tumor mass was reduced by 60% in the therapeutic protocol and 80-90% in the suppressive protocol (**Fig 1B**). A similar level of proteasome inhibition was observed in the cell preparations of lungs at 4 h after treatments, with no inhibition apparent in the tissues tested after 18 h (data not shown). Further, the Bzb-T regimen had no significant effects either on total leukocyte counts in control or tumor-draining LN, tumor-infiltrating lymphocytes, and spleen, or in subsets of $CD4^+$T, $CD8^+$T and $CD11c^+$ cells (**Fig 1C, D, E**) or in DX-5^+ NK cells (data not shown) analyzed in the tumor-draining LN on day 13 at 4 h after last bortezomib injection. In contrast, the suppressive Bzb-S regimen resulted in a leukocytopenia (**Fig 1C, D, E**), which may explain why bortezomib given at the time of allogeneic bone marrow transfer in mice attenuates acute GVHD (10).

Effect of bortezomib treatment on antigen presentation *in vitro* and *in vivo*

Since activity of the cellular proteasome is required to process antigens for presentation to T-cells, we assessed whether bortezomib might affect the ability of antigen-presenting cells to present antigen. We thus purified $CD11c^+$ cells *ex vivo* from the spleen of mice (with no tumor injection) treated with either Bzb-T or Bzb-S regimens, and analyzed their capacity to process whole HA protein, pulsed by a noncovalent cationic Pro-Ject intracellular delivery reagent, and cross-present HA peptides to cognate $CD8^+$ T-cells *in vitro*. Following a co-culture of equal numbers of these purified $CD11c^+$ cells from various groups of mice with a fixed number of TCRHA Cln4 $CD8^+$ T cells for 3 days, we observed no differences in T-cell proliferation or IFNγ production. This suggested no reduction of antigen presentation on a per-cell basis by isolated splenic $CD11c^+$ cells from the mice treated with the Bzb-T or Bzb-S regimens (**Fig 2**). Thus, the cellular antigen presentation *per se* was not affected by bortezomib even though the total number of $CD11c^+$ cells would be lower in mice treated with the suppressive Bzb-S regimen as per Figure 1. Therefore, under these assay conditions, bortezomib has no major suppressive effect on T-cell function following HA antigen processing or presentation assessed *in vitro*.

Using the two experimental regimens of bortezomib administration, we also assessed HA antigen-specific proliferation of transferred $CD4^+$ and $CD8^+$ TCRHA T-cells as a read out of the efficiency of class I and class II antigen presentation in an adoptive cell transfer setting *in vivo*. Lymphodeficient $RAG^{-/-}$ mice reconstituted with CFSE-labeled TCRHA $6.5^{+/+}$ $CD4^+$ or Cln4 $CD8^+$ T-cells were injected with RencaHA tumor cells and the Bzb-T and Bzb-S regimens were started on the same day (day 0) as shown in **Fig 2B**. The HA-specific T-cell proliferation on day 4 in the LN draining to the site of injected tumor cells following therapeutic Bzb-T or suppressive Bzb-S regimens compared well with the untreated tumor-bearing mice **(Fig 2C)** despite the 60-80% cellular proteasome inhibition (**Fig 1**). We observed a decreased yield of $V\beta8.1/2^+CD4^+$ and $V\beta8.1/2^+CD8^+$ cells in the tumor-draining LN of mice treated with Bzb-S regimen, but not with Bzb-T regimen, with little effect on T cell proliferation *per se*. Even using an injection regimen where bortezomib was started one day before tumor injection, or using irradiated tumor cells instead of live tumor cells, no suppressive effect of bortezomib on subsequent T-cell proliferation was observed (data not shown). Moreover, there was no effect of bortezomib treatment on the expression of costimulatory molecules CD80, CD86 or CD40 by CD11c^{high}MHCII^{high} cellular subsets in the tumor-draining LN (**Fig 2D**) or spleen (data not shown) from either of the regimens. Following only the suppressive Bzb-S regimen, a noticeable decrease was observed in the number of lymphoid tissue-resident subset of CD11c^{high}CD8^{high} DC expressing MHC II^{high} or co-stimulatory molecules CD80, CD86 and CD40 cells (**Fig 2E**). It is important to note that even though the residual numbers of CD11c^{high} CD8^{high}DC are low following the suppressive Bzb-S regimen, they showed no decrease in the relative level of expression of CD80, CD86 and CD40 molecules (**Fig 2D**), and no apparent decrease in CD4$^+$ or CD8$^+$ T cell proliferation following the Bzb-S regimen (**Fig 2C**). Thus, the effects of bortezomib appear merely quantitative and do not have a bearing on the maturation or antigen processing by CD11c^{high}CD8^{high} tissue-resident antigen presenting cells on a per-cell basis. Yet, if there is an excessive reduction in their numbers as it happens following the suppressive Bzb-S regimen, it may most likely compromise antitumor outcome. Indeed, treatment of mice with the Bzb-S (but not the Bzb-T) regimen immediately after injection of RencaHA cells substantially increased the number of metastases subsequently observed on day 14 (**Supplementary Fig 1**). This immunosuppressive effect resulted in increases in the number of lung metastases following the injection of RencaHA cells even 4 or 7 days after treatment with the Bzb-S regimen (**Supplementary Fig 2**). These data suggest that even though the suppressive Bzb-S regimen does not have a major effect on the maturation and antigen processing by individual DC *per se*, an excessive reduction in total DC numbers may still diminish antitumor immune effects *in vivo*. By contrast, the therapeutic Bzb-T regimen had no observable effects on lung metastases even when administered immediately after RencaHA injection (**Supplementary Fig 1 and 2**). Moreover, we also observed that tumor cells treated with bortezomib *in vitro* exhibit higher expression of calreticulin (**Supplementary Fig 3**). Increased cell surface calreticulin expression on tumor cells after bortezomib exposure could indicate “immunogenic cell death” so as to facilitate antigen uptake and presentation by DCs. These findings predict that the dose and regimen of bortezomib treatment is critical in deciding the outcome of antitumor immune response. Therefore, only the Bzb-T regimen was used in subsequent adoptive T-cell transfer experiments.

Sustained T-cell function *in vivo* following bortezomib treatment

We next investigated effects of bortezomib specifically on functional parameters of T-cell activation, proliferation and effector function *in vivo*. Following the establishment of palpable subcutaneous RencaHA or 4T1.2HA tumors ranging in size from 0.5 to 0.8 cm^3 in lymphodeficient RAG$^{-/-}$ mice, naïve CFSE-labeled TCRHA CD8$^+$ T-cells were transferred on day 6, followed by the Bzb-T regimen, and analyzed at 4 h or 24 h after last bortezomib treatment on day 9 as per the indicated scheme (**Fig 3A**). Following Bzb-T regimen, there was no statistically significant change in the total yield of K^d:HA tetramer$^+$ CD8$^+$ T-cells from the tumor-draining LN, nor was there a decrease or delay in HA-specific CD8$^+$ T-cell proliferation as analyzed on gated K^d:HA tetramer$^+$ T-cells in these mice either at 4 h or 24 h after last bortezomib injection (**Fig 3B**). A similar proliferation pattern was observed for HA-specific $CD4^+$ T-cells (data not shown). Rather, as analyzed on gated $CD8^+V\beta8.1/2^+$ cells in the draining LN of RencaHA or 4T1.2HA tumor-bearing $RAG^{-/-}$ mice on day 10, we observed that Bzb-T regimen led to an accumulation of intracellular $CD3\zeta^{high}$ cells in activated $CD25^+$ T-cell subset (**Fig 3C**). Zebra plots demonstrate a pronounced increase in the event density of $CD25^+$ T cells in the right quadrant when compared with untreated mice, suggesting stabilization of T-cell receptor CD3ζ in activated T-cells following Bzb-T regimen. We also investigated the influence of bortezomib regimen on the endogenous antitumor response in a polyclonal T-cell environment in the wild-type mice established with RencaHA or 4T1.2HA tumors and injected with Bzb-T regimen without any adoptive T-cell transfer as per the scheme shown in **Fig 3A**. Results show that in gated $CD8^+V\beta8.1/2^+$ T cells (frequency in the range of 8-10%) from the tumor-draining LN of wild-type mice, there is an enhanced secretion of intracellular IFNγ and CD3ζ expression following administration of the therapeutic regimen of Bzb-T in both RencaHA as well as in the aggressive breast adenocarcinoma model 4T1.2HA (**Fig 4A**). We also assessed immune cell viability by performing 7AAD staining along with CD3 or CD11c. Data reveal no increase in $7AAD^+$ cells either in CD3 or CD11c subsets, suggesting no loss of cell viability following the therapeutic Bzb-T regimen in the wild-type mice (**Fig 4B**). These data suggest that there is no suppression of endogenous T-cell response either in the monoclonal or polyclonal T-cell environment by the tested therapeutic regimen of bortezomib. Rather, it is evident that proteasome inhibition by bortezomib stabilizes the T-cell receptor CD3ζ, and thereby sustains the T-cell activation signals.

To determine any effect of bortezomib on the cytotoxic function of activated T-cells, we evaluated the ability of transferred TCRHA $CD8^+$CTLs to kill HA-expressing target cells in presence of bortezomib using an *in vivo* CTL assay. No reduction in HA-specific lysis was observed by CTLs in bortezomib-administered mice (**Fig 4C**). To further elaborate on the underlying mechanisms of the observed T-cell effects, we investigated the influence of bortezomib on NFκB activation downstream of CD3ζ signaling. NFκB is a "rapid-acting" primary transcription factor that does not require new protein synthesis in order to become activated and act as first responder in regulating various genes responsible for both the innate and adaptive immune cell proliferation and effector function. Purified $CD8^+$T cells treated *in vitro* with bortezomib (10 nM) for 4 h showed an increase in the phosphorylation of p65 in both nuclear and cytoplasmic fractions (**Fig 4D**), suggesting that bortezomib promotes NFκB activation in T-cells. Taken together, these data show that bortezomib has no discernible immunosuppressive consequences on T-cell function *in vivo* following the tested Bzb-T regimen in contrast to *in vitro* studies on human myeloid dendritic cells and NK cells (9,12,14).

Adoptive T-cell transfer in combination with bortezomib administration results in reduced lung metastases and enhanced survival

The adoptive transfer of T-cells could provide a natural source of multiple death ligands (FasL, TRAIL, TNF etc) for cancer therapy at the tumor site. Recent studies have illustrated that adoptive T-cell transfer provides the maximal therapeutic benefit when a lymphocyte depleting pre-conditioning regimen is used and less differentiated naïve $CD8^+$T-cells (T_N)

are transferred (29). Therefore, we investigated the effects of bortezomib administration combined with adoptive transfer of CD8 T_N cells in lymphodeficient RAG2$^{-/-}$ mice with a large established (7 day) lung tumor burdens of RencaHA cells as per the indicated schemes (**Fig 5A, C**). No difference in the immunohistological staining for CD3 was seen in lung tumor nodules following T_N cell transfer in the presence or absence of bortezomib treatment (**Fig 5B**) suggesting that bortezomib had no noticeable detrimental effect on T-cell migration and infiltration of the lung tumor mass. Moreover, in tumor-bearing mice treated with bortezomib (1 mg/kg body weight, approximately 20 nM) alone, there was little effect on the large number of tumor metastases with mice exhibiting numerous pulmonary tumor nodules (mean 442 ± 184 SD per mouse) close to the range of saline controls (753 ± 438) (**Fig 5A** and **6A**). TCRHA CD8 T_N cell transfer reduced the nodule count to a mean of 144 ± 103 per mouse. The tumor nodule count was further significantly reduced to a mean of just 25 ± 34 when bortezomib was administered 3 days after T_N cell transfer (**Fig 5A** and **6A**). Interestingly, a 3-week therapy regimen of bortezomib post T_N cell transfer, similar to the combination regimen of bortezomib and TRAIL receptor agonist mAb we used previously (7), significantly enhanced survival with 40% of mice still alive after a 90-day observation period (**Fig 5C)**.

Immunohistochemical analyses of lungs from mice treated with bortezomib alone or saline showed numerous large tumor nodules with prominent proliferating cell nuclear antigen (PCNA) staining in contrast to lungs from tumor-bearing mice treated with T_N cells or a combination of T_N cells and bortezomib (**Fig 6A**). Moreover, increased apoptosis as evaluated by TUNEL staining was observed in lungs of tumor-bearing mice treated with a combination of T_N cells and bortezomib compared with other groups (**Fig 6B**). We speculate that increased apoptosis at the site of tumor may increase the availability of tumor antigens, and thus enhance tumor control by T-cell therapy as observed in our combination regimen. We also tested whether the observed therapeutic effect could be ascribed to bortezomib's influence on tumor vasculature and stromal cells as suggested elsewhere (30-32). We did not observe major change in numbers of vascular endothelial cells in bortezomib-treated mice when compared with untreated mice. However, based on staining pattern for the vascular endothelial cell marker CD34 in the lungs of tumor-bearing mice treated with bortezomib, the global architecture of the tumor looked different, suggesting some effects on tumor vasculature following bortezomib regimen (**Fig 6C**).

Bortezomib improves T-cell therapy by sensitizing tumors to the FasL lytic pathway

Although we observed a stabilized expression of MHC molecules on RencaHA tumor cells *ex vivo* from mice administered with the Bzb-T regimen, the expression of Fas receptor on MHC-I K^{d+} tumor cells increased from 67% to 96% in mice treated with Bzb-T regimen when compared with untreated mice (**Fig 7A**). We also noted that various tumor cells including RencaHA, breast 4T1, colon C26, and lymphoma A20 that showed upregulated Fas expression following overnight treatment with bortezomib (20 nM) *in vitro* (data not shown), all exhibited enhanced sensitivity to lysis by recombinant FasL molecules (**Fig 7B**). Moreover, these tumor cells were also more sensitive to death ligand-mediated lysis by T-cells, since various bortezomib-treated cancer cells loaded with HA peptide (10^{-6} M) were very efficiently killed by TCRHA Cln4 Pfp$^{-/-}$ CTLs, which utilize the FasL but not the perforin-dependent granule exocytosis lytic pathway (**Fig 7C**). This FasL-mediated tumor cell lysis was necessary for the antitumor effects of adoptively transferred T-cells *in vivo* since adoptive transfer of *in vitro* activated Cln4 gld.gld CTLs, which lacked functional FasL, to RAG2$^{-/-}$ mice injected with RencaHA tumor cells i.v. resulted in a significantly greater number of pulmonary tumor nodules when compared with mice receiving Cln4 Pfp$^{-/-}$ CTLs or Cln4 CTLs (**Fig 7D**), even though different CTL produced similar amounts of IFNγ (data not shown). These results suggest that the FasL pathway is critical for tumor clearance following bortezomib administration in those tumors that express Fas. Indeed, therapeutic benefit of the combination of adoptive TCRHA T_N cell transfer and bortezomib was almost completely blocked by the administration of a FasL-neutralizing antibody in the RencaHA model (**Fig 7E**). We also noted upregulated Fas expression in human melanoma tissue sections (**Fig 7F**) from one responding advanced-stage (III or IV) metastatic melanoma patient, who showed a partial response of 8 months following treatment with a combination of an alkylating drug temozolomide and bortezomib in a phase I clinical trial (26).

Discussion

We investigated the effects of bortezomib administration on adoptive T-cell transfers in lymphodeficient RAG2$^{-/-}$ mice with established RencaHA tumors and designed *in vivo* protocols to examine MHC class I and II-restricted antigen presentation, dendritic cell function, T-cell activation and proliferation, and lysis of specific targets. Adoptive T-cell transfer followed by a tested therapeutic regimen of bortezomib resulted in a reduction in lung tumor nodules and enhanced survival. Taken together, our data suggest that T-cell function is sustained *in vivo* following administration of the therapeutic regimen of bortezomib when compared with a suppressive regimen close to the maximal tolerated levels for this drug. These findings provide evidence that, with appropriate timing and dosing of bortezomib, a significant level of therapeutic benefit can be achieved by combining the drug with adoptive T-cell therapy for the treatment of solid tumors.

Bortezomib can have multiple direct effects on tumor cells including disruption of DNA damage repair pathways, increased calcium levels (33), endoplasmic reticulum stress, aggresome formation (34), and alterations in mitochondrial function (33). In addition to direct anti-tumor effects, bortezomib can also have immunostabilizing effects on host immune system. Chang *et al* observed that treatment of ovarian tumor cells with bortezomib led to the upregulation of hsp60 and hsp90 on the cell surface and promoted their phagocytosis by dendritic cells. Expression of heat-shock proteins on ovarian tumor cells is an important determinant of whether bortezomib-treated tumor cells can generate tumor-specific CD8 T-cells. In addition, dendritic cells that were treated with bortezomib *in vitro* showed increased maturation, which resulted in potent immune-mediated antitumor effects (18). It is also reported that bortezomib induces apoptosis in immature DCs, but to a much lesser extent in mature DCs (35). Bortezomib enhanced antigen-specific cytotoxic T-cell responses against immune-resistant cancer cells generated by STAT3-ablated dendritic cells (36). Also, bortezomib could restore MART-1 antigen expression on human melanoma cells to sensitize them to specific CTLs *in vitro* (37). It is worth noting that bortezomib inhibits inducible NFκB activity, but can activate constitutive NF-κB activity by triggering phosphorylation of IκB kinase and its upstream receptor-interacting protein 2, thereby enhancing cytotoxicity in multiple myeloma cells (38). Our data also suggest that bortezomib sustained FasL-mediated T-cell cytotoxicity either by stabilizing expression of IL-2 receptor-α chain and intracellular T-cell receptor CD3ζ and IFNγ in T-cells of tumor-bearing mice via increased phosphorylation of nuclear and cytoplasmic NFκB p65 levels in $CD8^+$ T-cells or by inhibiting their proteasomal degradation. In line with our observations, another study demonstrated differential effects of bortezomib on NFκB activity depending on different cell types: bortezomib triggered NFκB activity via the canonical pathway in peripheral blood mononuclear cells by enhancing non-proteosomal degradation of IκBα while NFκB activation was inhibited in bone marrow-derived stromal cells [39].

Conversely, some studies report on bortezomib's immunosuppressive effects. Bortezomib has been shown to reduce total numbers of dendritic cells and leukocytes in hosts (39), as also shown by the suppressive regimen of bortezomib we tested. Multiple administrations of bortezomib have also been found to limit anti-viral responses *in vivo* (40). Nencioni *et al* observed that exposure of dendritic cells to bortezomib reduces their phagocytic capacity. DCs treated with bortezomib showed skewed phenotypic maturation in response to stimuli of bacterial and endogenous sources, as well as reduced cytokine production and immunostimulatory capacity. DC migratory capabilities were also impaired following bortezomib treatment. Bortezomib was also seen to down-regulate MyD88, an essential adaptor for TLR signaling, and to relieve LPS-induced activation of NF-κB, IRF-3, and IRF-8 and of the MAP kinase pathway, and it was suggested that bortezomib could prove useful for tuning TLR signaling and for the treatment of inflammatory and immune-mediated disorders (39). It should be noted that in these studies, where bortezomib is deemed immunosuppressive, the concentrations of bortezomib used to derive these findings were high. The majority of these studies used 100–1000 nM concentrations of bortezomib *in vitro*; doses that cannot be extrapolated to the therapeutic situation *in vivo*. Only 10–20 nM concentrations of bortezomib are attainable *in vivo* (41), and the level of proteasome inhibition that occurs at these concentrations can be tolerated in both mice and humans without appreciable toxicity (42,43).

Therefore, appropriate timing and dosing of bortezomib is critical in order to optimize any immunotherapeutic effects while minimizing immunosuppression. This is evident from our data where combination of adoptive T-cell transfer with bortezomib resulted in diminished pulmonary tumor metastases and enhanced survival. In contrast to bortezomib's influence on tumor vasculature and stromal cells reported earlier (30-32), we found no major change in numbers of vascular endothelial cells in the lungs with tumor-metastases. However, based on CD34 staining pattern the global architecture of the tumor looked different, suggesting some effects on tumor vasculature following bortezomib regimen. Although we cannot rule out whether disruption of vascular integrity in the bortezomib-treated groups of tumor-bearing mice contributed to the therapeutic benefits that followed T-cell and bortezomib therapy, we noted a direct role of FasL-mediated clearance of tumor cells as supported by: (a) upregulation of Fas on tumor cells analyzed *ex vivo* from mice administered with bortezomib, (b) higher sensitivity of bortezomib-treated tumor cells *in vitro* to recombinant FasL molecules or $PfP^{-/-}$ CTLs, which utilize only the FasL pathway, (c) greater frequency of pulmonary tumor nodules in tumor-bearing mice transferred with gld.gld CTLs, which lack functional FasL pathway, and (d) blockade of therapeutic benefit of T-cells and bortezomib by FasL-neutralizing Ab administration in mice. Moreover, Fas upregulation on melanoma tissue correlated with better survival outcome in the single responding patient on a phase I clinical trial testing a combination of alkylating agent temozolomide and bortezomib in advanced-stage (III or IV) metastatic melanoma.

Endogenous cytokines may contribute to Fas up-regulation in tumor cells (44,45) following T-cell transfer and bortezomib therapy. We have also observed that at four hours following bortezomib administration to tumor-bearing mice, there is an elevation in serum levels of the immunostimulatory cytokines IL-2, IL-9, IL-12p40, IL-12p70, IL-15 and the chemokine RANTES (Pellom and Shanker, unpublished data) making it tempting to speculate that this enhanced inflammatory milieu may further prolong T-cell activation and sensitize tumor cells to cytolysis *in vivo*. Bortezomib can also maximize the apoptotic potential of cytokines on tumors (46). The sensitization of tumor cells to FasL pathway is particularly relevant in the context of immunoselection of antigen-deficient or low tumor cells. We previously reported that FasL cytolytic pathway played a dominant role in the T-cell-mediated eradication of Fas-sensitive Renca tumors presenting low levels of antigens following adoptive T-cell therapy (47). Also more recently, FasL-mediated immune surveillance by T-cells was found to be essential for the control of spontaneous B-cell lymphomas (48).

Second generation proteasome inhibitors such as carfilzomib (49), or the natural product withanolide E recently identified by us as a potent novel sensitizer of cancer cells to extrinsic apoptosis (50), which exhibit minimal toxic effects as single agents, might be even more therapeutically advantageous in combination with adoptive T-cell transfer. Preclinical studies testing these agents with adoptive T-cell transfer are currently underway. In summary, our study using the preclinical cancer models has provided both a molecular basis and a translationally-relevant proof of principle that the therapeutic combination of adoptive T-cell therapy with agents that sensitize cancer cells to apoptosis may further improve responses to adoptive T-cell transfer.

Supplementary Material

Refer to Web version on PubMed Central for supplementary material.

Acknowledgments

Financial support: This project has been funded in whole or in part with federal funds to TJS from the National Cancer Institute, National Institutes of Health (NIH), under contracts N01-CO-12400 and HHSN261200800001E. This work was also supported by funds to AS from the NIH grants U54 CA163069, SC1 CA182843, U54 MD007593 and R01 CA175370. STP was supported by NIH training grants T32 5T32HL007737 and R25 GM059994. The Meharry Morphology and Flow Cytometry Cores are supported by NIH grants G12 MD007586, R24 DA036420 and S10 RR0254970. The content of this publication does not necessarily reflect the views or policies of the Department of Health and Human Services, nor does mention of trade names, commercial products, or organizations imply endorsement by the US Government. This Research was also supported [in part] by the Intramural Research Program of NIH, Frederick National Lab, Center for Cancer Research.

We thank D. Haines, L. Sherman, H. Levitsky, J. Yewdell, S. Durum, A. Richmond and D. Forbes for helpful feedback.

References

1. Driscoll JJ, Dechowdhury R. Therapeutically targeting the SUMOylation, Ubiquitination and Proteasome pathways as a novel anticancer strategy. Target Oncol. 2010; 5(4):281–9. [PubMed: 21125340]
2. Bross PF, Kane R, Farrell AT, Abraham S, Benson K, Brower ME, et al. Approval summary for bortezomib for injection in the treatment of multiple myeloma. Clinical cancer research : an official journal of the American Association for Cancer Research. 2004; 10(12 Pt 1):3954–64. [PubMed: 15217925]
3. Kane RC, Dagher R, Farrell A, Ko CW, Sridhara R, Justice R, et al. Bortezomib for the treatment of mantle cell lymphoma. Clinical cancer research : an official journal of the American Association for Cancer Research. 2007; 13(18 Pt 1):5291–4. [PubMed: 17875757]
4. Li T, Ho L, Piperdi B, Elrafei T, Camacho FJ, Rigas JR, et al. Phase II study of the proteasome inhibitor bortezomib (PS-341, Velcade) in chemotherapy-naive patients with advanced stage non-small cell lung cancer (NSCLC). Lung Cancer. 2010; 68(1):89–93. [PubMed: 19524318]
5. Sayers TJ, Brooks AD, Koh CY, Ma W, Seki N, Raziuddin A, et al. The proteasome inhibitor PS-341 sensitizes neoplastic cells to TRAIL-mediated apoptosis by reducing levels of c-FLIP. Blood. 2003; 102(1):303–10. [PubMed: 12637321]
6. Johnson TR, Stone K, Nikrad M, Yeh T, Zong WX, Thompson CB, et al. The proteasome inhibitor PS-341 overcomes TRAIL resistance in Bax and caspase 9-negative or Bcl-xL overexpressing cells. Oncogene. 2003; 22(32):4953–63. [PubMed: 12902978]
7. Shanker A, Brooks AD, Tristan CA, Wine JW, Elliott PJ, Yagita H, et al. Treating metastatic solid tumors with bortezomib and a tumor necrosis factor-related apoptosis-inducing ligand receptor agonist antibody. J Natl Cancer Inst. 2008; 100(9):649–62. [PubMed: 18445820]
8. Brooks AD, Jacobsen KM, Li W, Shanker A, Sayers TJ. Bortezomib sensitizes human renal cell carcinomas to TRAIL apoptosis through increased activation of caspase-8 in the death-inducing signaling complex. Molecular cancer research : MCR. 2010; 8(5):729–38. [PubMed: 20442297]
9. Nencioni, A.; Garuti, A.; Schwarzenberg, K.; Cirmena, G.; Dal Bello, G.; Rocco, I., et al. Proteasome inhibitor-induced apoptosis in human monocyte-derived dendritic cells. Vol. 36. WILEY-VCH Verlag; 2006. p. 681-89.
10. Sun K, Welniak LA, Panoskaltsis-Mortari A, O'Shaughnessy MJ, Liu H, Barao I, et al. Inhibition of acute graft-versus-host disease with retention of graft-versus-tumor effects by the proteasome inhibitor bortezomib. Proc Natl Acad Sci U S A. 2004; 101(21):8120–5. [PubMed: 15148407]
11. Berges C, Haberstock H, Fuchs D, Miltz M, Sadeghi M, Opelz G, et al. Proteasome inhibition suppresses essential immune functions of human CD4+ T cells. Immunology. 2008; 124(2):234–46. [PubMed: 18217957]
12. Feng X, Yan J, Wang Y, Zierath JR, Nordenskjold M, Henter JI, et al. The proteasome inhibitor bortezomib disrupts tumor necrosis factor-related apoptosis-inducing ligand (TRAIL) expression and natural killer (NK) cell killing of TRAIL receptor-positive multiple myeloma cells. Mol Immunol. 2010; 47(14):2388–96. [PubMed: 20542572]
13. Heider U, Rademacher J, Kaiser M, Kleeberg L, von Metzler I, Sezer O. Decrease in CD4+ T-cell counts in patients with multiple myeloma treated with bortezomib. Clin Lymphoma Myeloma Leuk. 2010; 10(2):134–7. [PubMed: 20371447]
14. Straube C, Wehner R, Wendisch M, Bornhauser M, Bachmann M, Rieber EP, et al. Bortezomib significantly impairs the immunostimulatory capacity of human myeloid blood dendritic cells. Leukemia. 2007; 21(7):1464–71. [PubMed: 17495970]
15. Zinser E, Rossner S, Littmann L, Luftenegger D, Schubert U, Steinkasserer A. Inhibition of the proteasome influences murine and human dendritic cell development in vitro and in vivo. Immunobiology. 2009; 214(9-10):843–51. [PubMed: 19628298]
16. Ames E, Hallett WH, Murphy WJ. Sensitization of human breast cancer cells to natural killer cell-mediated cytotoxicity by proteasome inhibition. Clin Exp Immunol. 2009; 155(3):504–13. [PubMed: 19220837]
17. Armeanu S, Krusch M, Baltz KM, Weiss TS, Smirnow I, Steinle A, et al. Direct and natural killer cell-mediated antitumor effects of low-dose bortezomib in hepatocellular carcinoma. Clinical

cancer research : an official journal of the American Association for Cancer Research. 2008; 14(11):3520–8. [PubMed: 18519785]

18. Chang CL, Hsu YT, Wu CC, Yang YC, Wang C, Wu TC, et al. Immune mechanism of the antitumor effects generated by bortezomib. J Immunol. 2012; 189(6):3209–20. [PubMed: 22896634]
19. Lundqvist A, Yokoyama H, Smith A, Berg M, Childs R. Bortezomib treatment and regulatory T-cell depletion enhance the antitumor effects of adoptively infused NK cells. Blood. 2009; 113(24): 6120–7. [PubMed: 19202127]
20. Seeger JM, Schmidt P, Brinkmann K, Hombach AA, Coutelle O, Zigrino P, et al. The proteasome inhibitor bortezomib sensitizes melanoma cells toward adoptive CTL attack. Cancer research. 2010; 70(5):1825–34. [PubMed: 20179203]
21. Shi J, Tricot GJ, Garg TK, Malaviarachchi PA, Szmania SM, Kellum RE, et al. Bortezomib down-regulates the cell-surface expression of HLA class I and enhances natural killer cell-mediated lysis of myeloma. Blood. 2008; 111(3):1309–17. [PubMed: 17947507]
22. Spisek R, Charalambous A, Mazumder A, Vesole DH, Jagannath S, Dhodapkar MV. Bortezomib enhances dendritic cell (DC)-mediated induction of immunity to human myeloma via exposure of cell surface heat shock protein 90 on dying tumor cells: therapeutic implications. Blood. 2007; 109(11):4839–45. [PubMed: 17299090]
23. Morgan DJ, Kreuwel HT, Fleck S, Levitsky HI, Pardoll DM, Sherman LA. Activation of low avidity CTL specific for a self epitope results in tumor rejection but not autoimmunity. J Immunol. 1998; 160(2):643–51. [PubMed: 9551898]
24. Kirberg J, Baron A, Jakob S, Rolink A, Karjalainen K, von Boehmer H. Thymic selection of CD8+ single positive cells with a class II major histocompatibility complex-restricted receptor. The Journal of experimental medicine. 1994; 180(1):25–34. [PubMed: 8006585]
25. Kreuwel HT, Morgan DJ, Krahl T, Ko A, Sarvetnick N, Sherman LA. Comparing the relative role of perforin/granzyme versus Fas/Fas ligand cytotoxic pathways in CD8+ T cell-mediated insulin-dependent diabetes mellitus. J Immunol. 1999; 163(8):4335–41. [PubMed: 10510373]
26. Su Y, Amiri KI, Horton LW, Yu Y, Ayers GD, Koehler E, et al. A phase I trial of bortezomib with temozolomide in patients with advanced melanoma: toxicities, antitumor effects, and modulation of therapeutic targets. Clinical cancer research : an official journal of the American Association for Cancer Research. 2010; 16(1):348–57. [PubMed: 20028756]
27. Chakraborty M, Abrams SI, Coleman CN, Camphausen K, Schlom J, Hodge JW. External beam radiation of tumors alters phenotype of tumor cells to render them susceptible to vaccine-mediated T-cell killing. Cancer Res. 2004; 64(12):4328–37. [PubMed: 15205348]
28. Seki N, Brooks AD, Carter CR, Back TC, Parsoneault EM, Smyth MJ, et al. Tumor-specific CTL kill murine renal cancer cells using both perforin and Fas ligand-mediated lysis in vitro, but cause tumor regression in vivo in the absence of perforin. J Immunol. 2002; 168(7):3484–92. [PubMed: 11907109]
29. Klebanoff CA, Gattinoni L, Restifo NP. Sorting through subsets: which T-cell populations mediate highly effective adoptive immunotherapy? J Immunother. 2012; 35(9):651–60. [PubMed: 23090074]
30. Liesveld JL, Rosell KE, Lu C, Bechelli J, Phillips G, Lancet JE, et al. Acute myelogenous leukemia--microenvironment interactions: role of endothelial cells and proteasome inhibition. Hematology. 2005; 10(6):483–94. [PubMed: 16321813]
31. Goffin L, Seguin-Estevez Q, Alvarez M, Reith W, Chizzolini C. Transcriptional regulation of matrix metalloproteinase-1 and collagen 1A2 explains the anti-fibrotic effect exerted by proteasome inhibition in human dermal fibroblasts. Arthritis Res Ther. 2010; 12(2):R73. [PubMed: 20429888]
32. Kukreja A, Hutchinson A, Mazumder A, Vesole D, Angitapalli R, Jagannath S, et al. Bortezomib disrupts tumour-dendritic cell interactions in myeloma and lymphoma: therapeutic implications. Br J Haematol. 2007; 136(1):106–10. [PubMed: 17222199]
33. Landowski TH, Megli CJ, Nullmeyer KD, Lynch RM, Dorr RT. Mitochondrial-mediated disregulation of Ca2+ is a critical determinant of Velcade (PS-341/bortezomib) cytotoxicity in myeloma cell lines. Cancer research. 2005; 65(9):3828–36. [PubMed: 15867381]

34. Nawrocki ST, Carew JS, Pino MS, Highshaw RA, Andtbacka RH, Dunner K Jr. et al. Aggresome disruption: a novel strategy to enhance bortezomib-induced apoptosis in pancreatic cancer cells. Cancer research. 2006; 66(7):3773–81. [PubMed: 16585204]
35. Subklewe M, Sebelin-Wulf K, Beier C, Lietz A, Mathas S, Dorken B, et al. Dendritic cell maturation stage determines susceptibility to the proteasome inhibitor bortezomib. Human immunology. 2007; 68(3):147–55. [PubMed: 17349869]
36. Kim JE, Jin DH, Lee WJ, Hur D, Wu TC, Kim D. Bortezomib enhances antigen-specific cytotoxic T cell responses against immune-resistant cancer cells generated by STAT3-ablated dendritic cells. Pharmacological research : the official journal of the Italian Pharmacological Society. 2013; 71:23–33.
37. Jazirehi AR, Economou JS. Proteasome inhibition blocks NF-kappaB and ERK1/2 pathways, restores antigen expression, and sensitizes resistant human melanoma to TCR-engineered CTLs. Molecular cancer therapeutics. 2012; 11(6):1332–41. [PubMed: 22532603]
38. Hideshima T, Ikeda H, Chauhan D, Okawa Y, Raje N, Podar K, et al. Bortezomib induces canonical nuclear factor-kappaB activation in multiple myeloma cells. Blood. 2009; 114(5):1046–52. [PubMed: 19436050]
39. Nencioni A, Schwarzenberg K, Brauer KM, Schmidt SM, Ballestrero A, Grunebach F, et al. Proteasome inhibitor bortezomib modulates TLR4-induced dendritic cell activation. Blood. 2006; 108(2):551–8. [PubMed: 16537813]
40. Basler M, Lauer C, Beck U, Groettrup M. The proteasome inhibitor bortezomib enhances the susceptibility to viral infection. J Immunol. 2009; 183(10):6145–50. [PubMed: 19841190]
41. Hideshima T, Richardson P, Chauhan D, Palombella VJ, Elliott PJ, Adams J, et al. The proteasome inhibitor PS-341 inhibits growth, induces apoptosis, and overcomes drug resistance in human multiple myeloma cells. Cancer research. 2001; 61(7):3071–6. [PubMed: 11306489]
42. Adams J, Palombella VJ, Sausville EA, Johnson J, Destree A, Lazarus DD, et al. Proteasome inhibitors: a novel class of potent and effective antitumor agents. Cancer research. 1999; 59(11): 2615–22. [PubMed: 10363983]
43. Lightcap ES, McCormack TA, Pien CS, Chau V, Adams J, Elliott PJ. Proteasome inhibition measurements: clinical application. Clin Chem. 2000; 46(5):673–83. [PubMed: 10794750]
44. Lee JK, Sayers TJ, Brooks AD, Back TC, Young HA, Komschlies KL, et al. IFN-gamma-dependent delay of in vivo tumor progression by Fas overexpression on murine renal cancer cells. J Immunol. 2000; 164(1):231–9. [PubMed: 10605016]
45. Peshes-Yaloz N, Rosen D, Sondel PM, Krammer PH, Berke G. Up-regulation of Fas (CD95) expression in tumour cells in vivo. Immunology. 2007; 120(4):502–11. [PubMed: 17343612]
46. Khan T, Stauffer JK, Williams R, Hixon JA, Salcedo R, Lincoln E, et al. Proteasome inhibition to maximize the apoptotic potential of cytokine therapy for murine neuroblastoma tumors. J Immunol. 2006; 176(10):6302–12. [PubMed: 16670342]
47. Shanker A, Brooks AD, Jacobsen KM, Wine JW, Wiltrout RH, Yagita H, et al. Antigen presented by tumors in vivo determines the nature of CD8+ T-cell cytotoxicity. Cancer research. 2009; 69(16):6615–23. [PubMed: 19654302]
48. Afshar-Sterle S, Zotos D, Bernard NJ, Scherger AK, Rodling L, Alsop AE, et al. Fas ligand-mediated immune surveillance by T cells is essential for the control of spontaneous B cell lymphomas. Nature medicine. 2014; 20(3):283–90.
49. Arastu-Kapur S, Anderl JL, Kraus M, Parlati F, Shenk KD, Lee SJ, et al. Nonproteasomal targets of the proteasome inhibitors bortezomib and carfilzomib: a link to clinical adverse events. Clinical cancer research : an official journal of the American Association for Cancer Research. 2011; 17(9):2734–43. [PubMed: 21364033]
50. Henrich CJ, Brooks AD, Erickson KL, Thomas CL, Bokesch HR, Tewary P, et al. Withanolide E sensitizes renal carcinoma cells to TRAIL-induced apoptosis by increasing cFLIP degradation. Cell death & disease. 2015; 6:e1666. [PubMed: 25719250]

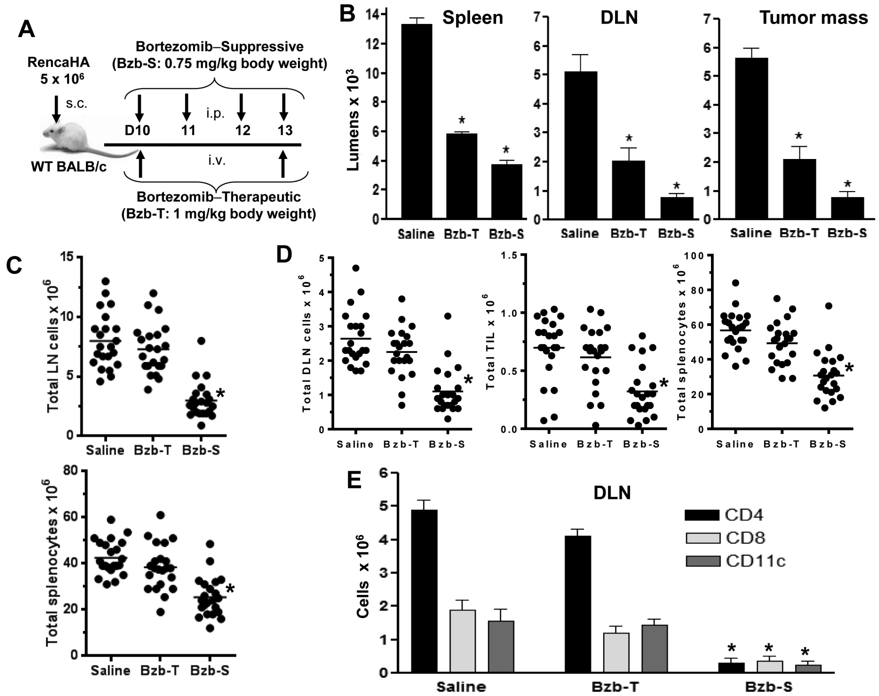

Figure 1. No major leukocytopenia following bortezomib's therapeutic regimen compared with the suppressive regimen *in vivo*

Subcutaneous tumors were allowed to establish in WT BALB/c mice following injection of 5×10^6 RencaHA tumor cells. On day 10, mice were injected with suppressive bortezomib (Bzb-S; 4 times a week) or therapeutic (Bzb-T; twice a week) regimens as indicated (***A***). ***B***, cellular proteasome activity in spleen, tumor-draining LN (DLN) and tumor mass was assayed at 4 h after last bortezomib administration by the luciferase-based enzymatic reaction. Data shown as mean luminescence ± SD from two independent experiments; $^*P < 0.001$ (two-sided unpaired *t* test) compared with saline, n = 4. Total cell counts of LN and spleen in mice with no tumor injection (***C***) or DLN, tumor-infiltrating lymphocytes (TIL), and spleen of tumor-bearing mice (***D***), or for $CD4^+$, $CD8^+$ and CD11c $^+$ cellular subsets in total leukocyte gates by flow cytometry in the DLN (***E***) analyzed at 4 h after last bortezomib injection. Data shown as mean values ± SD from six independent experiments; $^*p < 0.001$ (ANOVA, two-sided) compared with saline or Bzb-T; n = 22, each group.

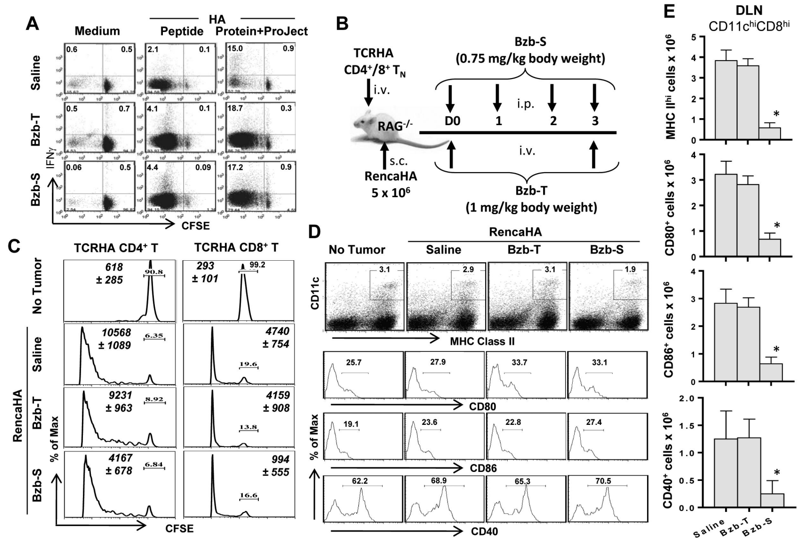

Figure 2. No diminution of antigen processing and cross-presentation by dendritic cells from bortezomib-treated mice

A, CD11c$^+$ cells were harvested *ex vivo* at 4 h after last bortezomib administration from the spleen of mice (with no tumor) treated according to the bortezomib regimens shown in Figure 1A. They were CD11c-labelled magnetic bead-purified, irradiated, and pulsed for 2 h with HA peptide (10^{-8} M) or with HA protein (10^{-8} M) along with Pro-Ject intracellular delivery reagent, and washed. Equal numbers of CD11c$^+$ cells from various groups of mice were co-cultured with CFSE-labeled RAG2$^{-/-}$Cln4 TCRHA CD8$^+$ T-cells for 3 days. CFSE versus IFNγ staining is shown on gated CD8$^+$H2:K^d-HA-tetramer$^+$ cells. Numbers in dot plots depict % positive cells. Representative data are shown from five independent experiments. ***B***, RAG$^{-/-}$ mice were reconstituted with TCRHA 6.5$^{+/+}$CD4$^+$ or RAG2$^{-/-}$Cln4 CD8$^+$ T-cells (5×10^6 i.v.) followed by injection of RencaHA tumor cells s.c. on the same day (day 0), when the bortezomib-therapeutic, Bzb-T, or suppressive, Bzb-S, regimens were also started according to the shown schedule. ***C***, HA antigen-specific proliferation of CFSE-labeled CD4$^+$ or CD8$^+$ TCRHA T-cells on day 4 in the tumor-draining LN is presented as readout of the efficiency of class I or class II antigen presentation. Numbers depict % undivided T-cells. Italicized numbers depict total Vβ8.1/2$^+$CD4$^+$ or Vβ8.1/2$^+$CD8$^+$ cells, respectively. Representative data are shown from three (CD4) or four (CD8) independent experiments. ***D***, expression of CD80, CD86 and CD40 on gated CD11c^{high}MHCII^{high} cells in the tumor-draining LN is shown. Numbers in dot plots and histograms depict % positive cells. Representative data are shown from three independent experiments. ***E***, total cell counts of CD11c^{high}CD8^{high} subset of DC in DLN expressing MHC II, CD80, CD86 or CD40 molecules. Data shown as mean values ± SD from three independent experiments; *$p < 0.001$ (ANOVA, two-sided) compared with saline or Bzb-T; n = 9, each group.

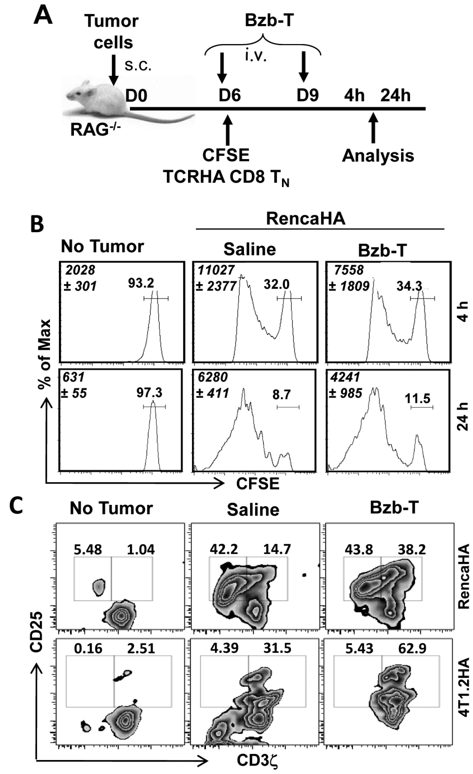

Figure 3. Sustained T-cell activity *in vivo* following the therapeutic regimen of bortezomib

CFSE-labeled naïve TCRHA RAG2$^{-/-}$Cln4 CD8 T-cells (5×10^6 i.v.) were transferred on day 6 when bortezomib regimen was started in RAG2$^{-/-}$ mice established with RencaHA (5×10^6) or 4T1.2HA (2×10^6) tumor cells according to the indicated schedule (***A***). ***B***, CFSE profile of CD8$^+$ TCRHA T-cells in the tumor-draining LN at 4 h or 24 h after last day 9 bortezomib injection. Italicized numbers in histograms depict total CD8$^+$H2:K^d-HA-tetramer$^+$ cells. Other numbers depict % positive cells. ***C***, intracellular CD3ζ versus surface CD25 staining in the tumor-draining LN on day 10 is shown on gated Cln4 TCR Vβ8.1$^+$CD8$^+$ cells. Numbers in dot plots depict % positive cells. Representative data shown from five (*B*), and seven (*C*) independent experiments.

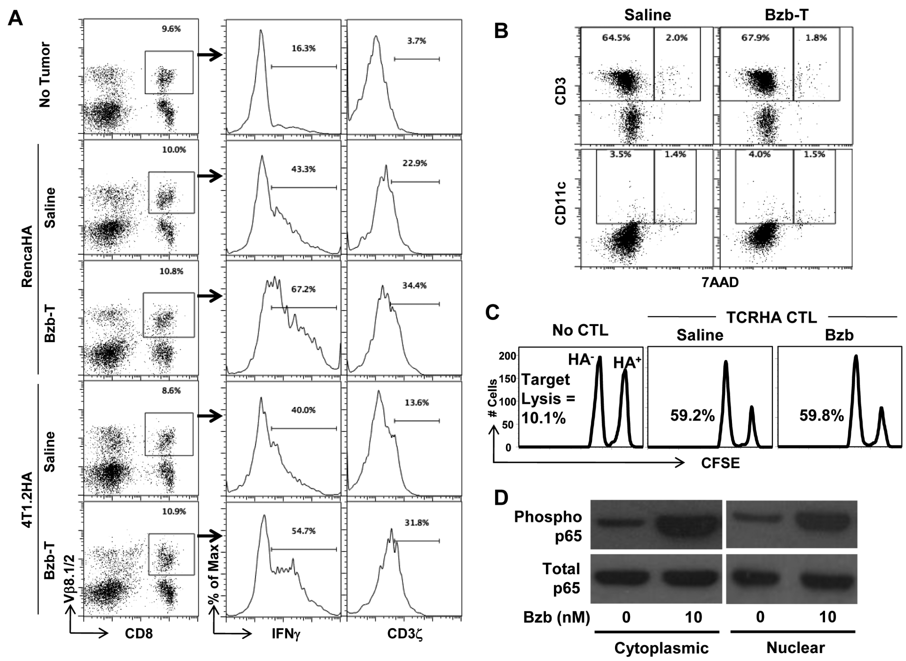

Figure 4. Endogenous T-cell activity *in vivo* following the therapeutic regimen of bortezomib

Bortezomib regimen was started on day 6 in wild-type mice established with RencaHA (5×10^6) or 4T1.2HA (2×10^6) subcutaneous tumors as per the schedule shown in Figure 3A. At 4 h after last day 9 bortezomib injection gated $CD8^+$ $V\beta8.1/2^+$ cells in the tumor-draining LN are analyzed for intracellular IFNγ and CD3ζ (***A***), or total tumor-draining LN cells analyzed for 7AAD versus surface CD3 or CD11c (***B)***. Numbers in dot plots or histograms depict % positive cells. ***C***, Total and phosphorylated forms of p65 are shown in the nuclear and cytoplasmic extracts of purified splenic $CD8^+$ T cells treated with 10 nM bortezomib for 4 h. ***D***, HA-specific lysis of HA-labeled ($CFSE^{high}$) or irrelevant NP-labeled ($CFSE^{low}$) splenocytes in bortezomib-administered syngeneic WT mice 18 h after transfer of *in vitro* activated TCRHA $CD8^+$ CTLs. Representative data shown from three (*A*, *B*, *C*, and *D*) independent experiments.

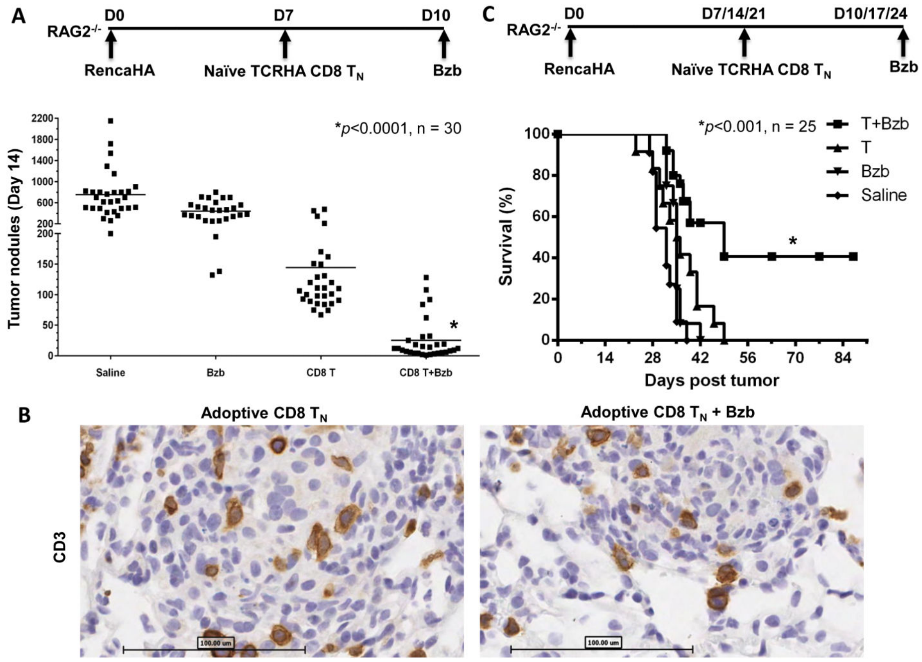

Figure 5. Undisturbed T-cell infiltration, reduced tumor nodules and enhanced survival following adoptive T-cell transfer combined with the therapeutic regimen of bortezomib

RAG2$^{-/-}$ mice were injected with RencaHA tumor cells (2 x10^{6} cells per mouse, i.v.) followed by naïve TCRHA RAG2$^{-/-}$Cln4 CD8 T-cells (0.5 × 10^{6} cells per mouse, i.v.) and bortezomib (1 mg/kg body weight, i.v.) as per the indicated regimens. ***A***, counts of pulmonary tumor nodules on day 14 after tumor injection. *, P<0.0001 (ANOVA, two-sided). ***B***, representative sections of lungs from RAG2$^{-/-}$ mice injected with the schedule shown in Figure 5A were stained on day 14 with CD3 Ab; n = 3, each group; bar = 100 μm. ***C*,** survival of RencaHA tumor-bearing RAG2$^{-/-}$mice. *, P<0.001 (two-sided log-rank test). The combination was compared with other groups, n = 30 (*A*) and 25 (*B*) from five independent experiments.

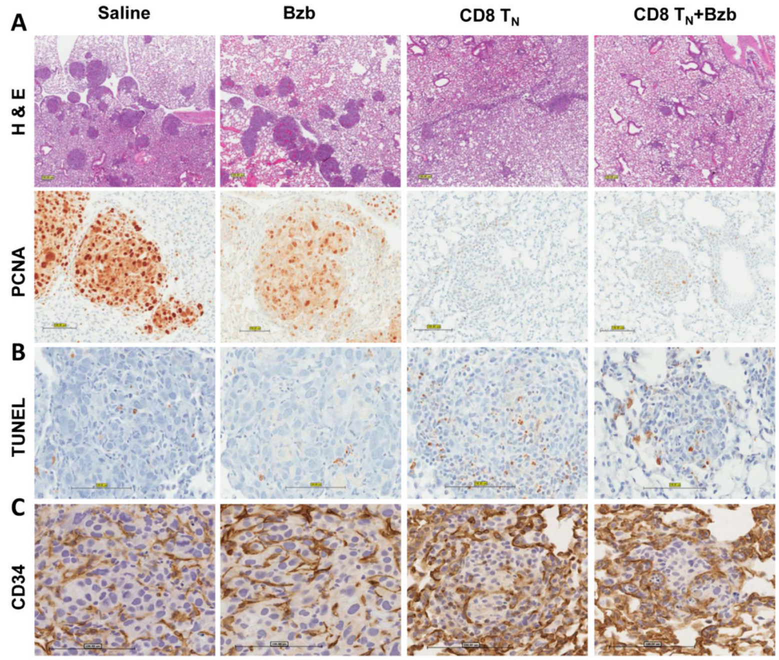

Figure 6. Increased apoptosis but not disruption of endothelium in the pulmonary tumor mass following adoptive T-cell transfer and therapeutic bortezomib regimen

Representative sections of lungs from RAG2$^{-/-}$ mice injected with RencaHA tumor cells, naïve TCRHA RAG2$^{-/-}$Cln4 CD8 T-cells and bortezomib as per schedule shown in Figure 5A were stained on day 14 with hematoxylin and eosin (H & E) (***A***), *PCNA*, proliferating cell nuclear antigen (***B***), *TUNEL*, terminal deoxynucleotidyl transferase dUTP nick end labeling (***C***), and CD34 Ab (***D***); n = 3, each group; bar = 100 µm, all images.

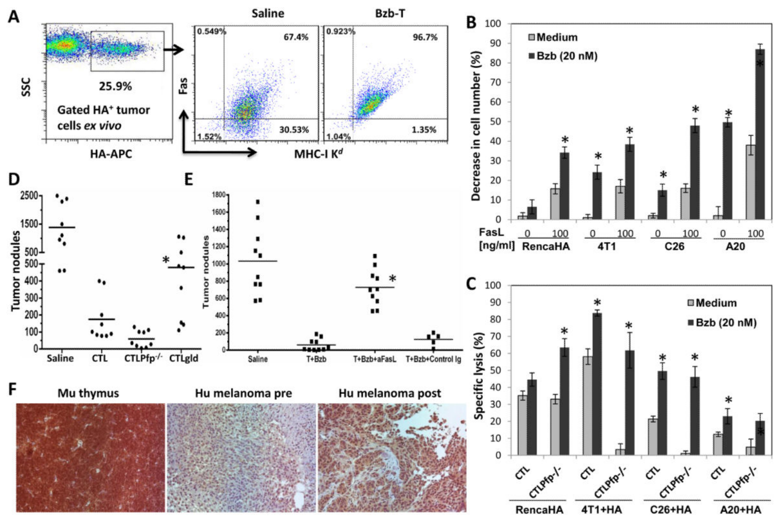

Figure 7. Bortezomib augments T-cell therapy by sensitizing tumors to FasL

A, MHC K^d versus Fas staining on gated HA^+ tumor cells harvested from mice administered with Bzb-T regimen. Numbers in dot plots represent % positive cells. Plots representative of two independent experiments. ***B***, percent decrease in cell number of RencaHA, 4T1, C26, and A20 tumor cells following overnight treatment with bortezomib (20 nM) and recombinant FasL molecules. *$P < 0.001$ (two-sided unpaired *t* test) compared with untreated samples. Data representative of three independent experiments. ***C***, percent specific lysis of bortezomib-treated RencaHA, 4T1, C26, and A20 tumor cells loaded with HA peptide (10^{-6} M) by TCRHA Cln4 or Cln4Pfp$^{-/-}$ CTLs. *$P < 0.001$ (two-sided unpaired *t* test) compared with untreated samples. Data representative of two independent experiments. ***D***, counts of pulmonary tumor nodules on day 14 in RAG2$^{-/-}$ mice injected with RencaHA tumor cells i.v. following adoptive transfer of 5×10^6 CTLs/mouse i.v. on day 10. Cln4 gld.gld CTLs were compared with Cln4 Pfp$^{-/-}$ CTLs or Cln4 CTLs. *$P < 0.001$ (ANOVA, two-sided), n = 9. Data representative of three independent experiments. ***E***, Counts of pulmonary tumor nodules on day 14 in RAG2$^{-/-}$ mice injected with RencaHA tumor cells i.v. following transfer of naïve Cln4 CD8 T-cells and bortezomib along with the administration of FasL neutralizing or isotype control antibody. *, $P<0.001$ (ANOVA, two-sided). The FasL neutralized group was compared with isotype IgG group, n = 10 from two independent experiments. ***F***, Fas expression analyzed using human and mouse cross-reactive CD95 antibody on human melanoma tissue sections from advanced-stage (III or IV) metastatic melanoma patients treated with a combination of temozolomide (50-75 mg/m^2) daily, orally, for 6 of 9 weeks and bortezomib (0.75-1.5 mg/m^2) by i.v. push on days 1, 4, 8, and 11 of every 21-d cycle. Paired pre (day 0) and post (day 45) treatment melanoma tissue samples from the sole responder patient are shown. Murine thymus is shown as a positive control for Fas staining. Magnification, 20x; Mu, murine; hu, human.